Bismuth-doped amorphous germanium sulfide semiconductors

K. L. Bhatia and D. P. Gosain
Department of Physics, Maharshi Dayanand University, Rohtak 124001, India

G. Parthasarathy and E. S. R. Gopal
Instrumentation and Services Unit, Indian Institute of Science, Bangalore 560012, India
(Received 6 February 1986; revised manuscript received 30 June 1986)

A study of the effect of bismuth dopant on the electronic transport properties of the amorphous semiconductors $Ge_{20}S_{80-x}Bi_x$ under high pressure (up to 140 kbar) has been carried out down to liquid-nitrogen temperature. The experiments reveal that the electronic conduction is strongly composition dependent and is thermally activated with a single activation energy at all pressures and for all compositions. A remarkable resemblance between the electronic conduction process, x-ray diffraction studies, and differential thermal analysis results is revealed. It is proposed that the n-type conduction in germanium chalcogenides doped with a large Bi concentration is due to the effect of Bi dopants on the positive correlation energy defects present in germanium chalcogenides. The impurity-induced chemical modification of the network creates a favorable environment for such an interaction.

I. INTRODUCTION

Germanium chalcogenide glassy semiconductors are an interesting and unique class of amorphous materials. They have a widely different lattice structure in crystalline and noncrystalline form. This is contrary to other vitreous semiconductors, which have similar short-range order in the two states.[1] Further, they have possible technical applications in electronic and optoelectronic devices.[2] Although chalcogenide glassy semiconductors are normally always p type and the added impurities do not alter its p-type conduction, a recent study has shown that the addition of Bi impurities in large concentrations (≥ 11 at.% in $Ge_{20}S_{80}$) can switch the conduction from p to n type.[3] The mechanism of such type of doping is not understood. The present paper is addressed to this aspect of the problem. We have been utilizing x-ray diffraction, differential thermal analysis, and the Bridgman anvil high-pressure technique to study the problem of doping of germanium chalcogenide glasses in depth.[4–10] In a recent Rapid Communication[4] we presented some preliminary results of our investigations. In this paper we are giving a detailed account of our investigations of the transport properties of amorphous $Ge_{20}S_{80-x}Bi_x$ ($x=0$, 4, 11, 15) under high pressure and down to liquid-nitrogen temperature. Results are discussed on the basis of a charged defect model of chalcogenide glasses. Some proposals regarding the mechanism of doping and the unique character of Bi dopants in germanium chalcogenides are put forward.

II. EXPERIMENTAL

The doped semiconducting vitreous materials $Ge_{20}S_{80-x}Bi_x$ ($x=0$, 4, 11, 15) are prepared by the conventional melt-quenching technique starting with proper quantities of high-purity elements (99.999%).[4] The characterization of the prepared glasses is carried out using x-ray diffraction and differential thermal analysis methods.[4]

The Bridgman anvil high-pressure technique and the apparatus for measurement of electrical transport are the same as explained in our earlier work.[4,11] Pressure contacts are used in electrical measurements and their ohmic nature is checked. When calculating the value of electrical resistivity at high pressures, changes in the sample dimensions are ignored. Steatite is used as a pressure transmitting medium. Silver chloride, which is a better transmitting medium, is not used because Ag is known to diffuse into the chalcogenide glasses, thus changing the electrical transport properties.[12]

III. RESULTS

The results of measurement of electrical resistivity at different pressures in $x=0$, 4, 11, and 15 compositions are presented in Fig. 1, which distinctly exhibits the presence of two pressure-induced sharp transitions in the region of (25–35)- and (75–80)-kbar pressure, respectively, in $x=11$ and $x=15$ compositions.[4] The pressure-induced effects in $x=4$ composition are surprising as there is only one sharp and relatively stronger transition around 80-kbar pressure where resistivity falls by about 7 orders of magnitude and thereafter the system behaves like a metal.[4] Pressure-induced effects in $x=0$ composition are altogether different from the doped systems. The temperature dependence of resistance of the $x=11$ and 15 samples after the second structural transformation [at (75–80)-kbar pressure] is shown in Fig. 2, which exhibits appropriate metallic behavior of the samples. $x=0$ and 4 samples at the same pressure (75 kbar) show semiconducting behavior.

The temperature dependence of electrical conductivity at different pressures in various compositions $Ge_{20}S_{80-x}Bi_x$ ($x=0$, 4, 11, 15) was also determined. Typical experimental results on $x=0$, 4, and 15 compositions are presented in Figs. 3–5, respectively. All four compositions studied exhibit appropriate thermally ac-

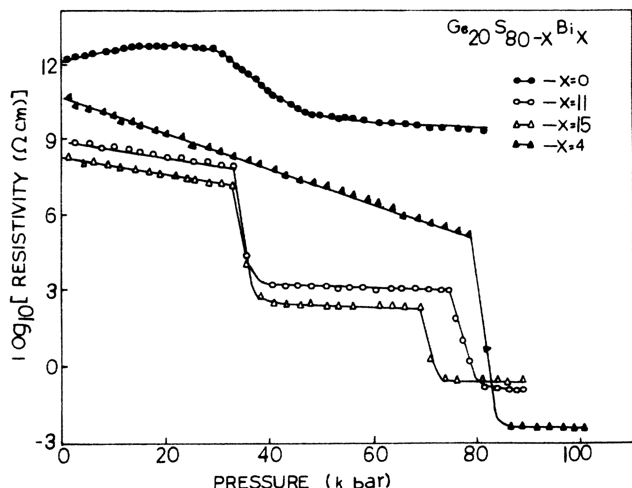

FIG. 1. Pressure dependence of the resistivity of $Ge_{20}S_{80-x}Bi_x$ ($x=0$, 4, 11, 15).

tivated electronic conduction at all pressures and follow the exponential relation:

$$\sigma=\sigma_0 \exp\left[-\frac{\Delta E}{k_B T}\right], \tag{1}$$

where ΔE is the activation energy and σ_0 is the preexponential factor. Values of various parameters (ΔE, σ_0, σ) of electrical conduction at different pressures are summarized in Table I. Figures 6 and 7 exhibit the pressure and composition dependence of the activation energy ΔE. These diagrams reveal two important and common features of the activation energy ΔE. Firstly, the pressure dependence of ΔE in $x=0$ and 4 compositions is similar whereas the behavior of ΔE in $x=11$ composition is similar to $x=15$ composition, but is different from its behavior in $x=0$ and 4 samples. Secondly, the composition dependence of ΔE exhibits a distinctive change in its

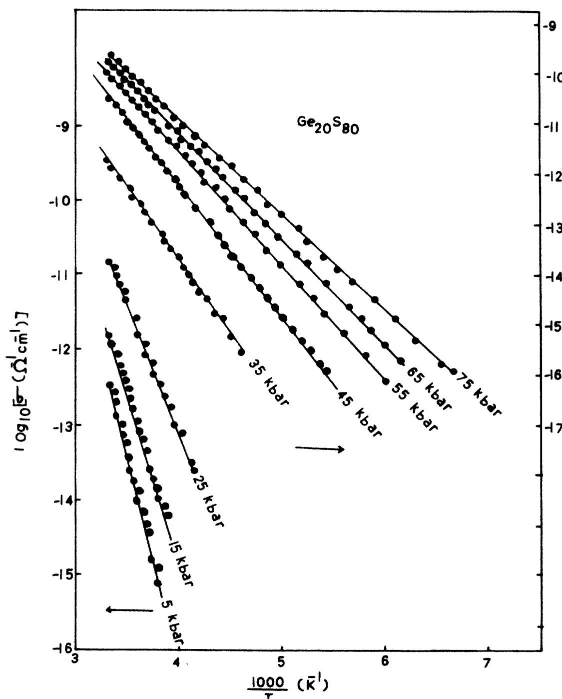

FIG. 3. Temperature-dependence conductivity of $Ge_{20}S_{80}$ at pressures of 5, 15, 25, 35, 45, 55, 65, and 75 kbar. The curves for 5, 15, and 25 kbar correspond to the left-hand side ordinate and the remaining curves correspond to the right-hand side ordinate. Ordinates of the curves for 5, 15, and 25 kbar are shifted successively by 1 order of magnitude.

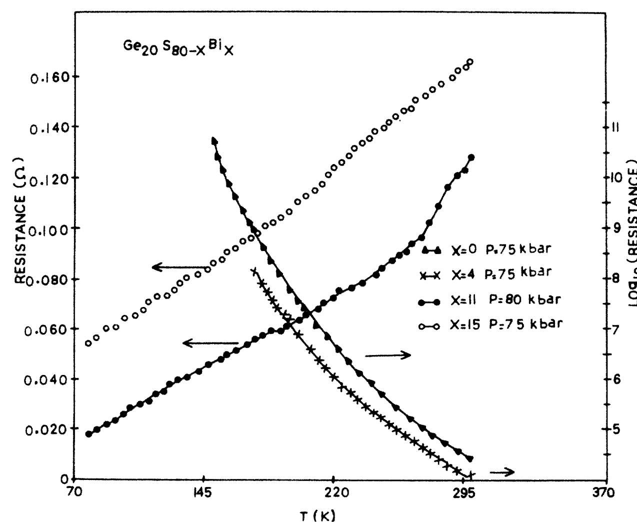

FIG. 2. (a) Temperature dependence of resistance of $x=11$ and 15 samples after the second structural transformation at 80- and 75-kbar pressure, respectively. (b) Temperature dependence of resistance of $x=0$ and 4 samples at the same pressure (75 kbar).

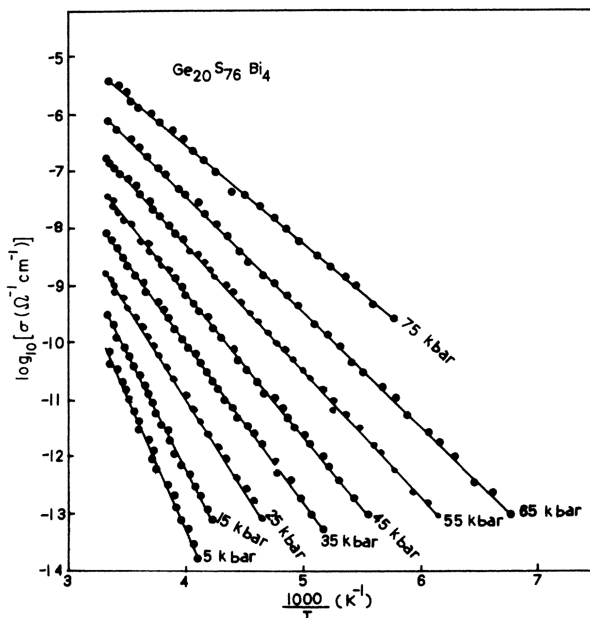

FIG. 4. Temperature-dependence conductivity of $Ge_{20}S_{76}Bi_4$ at pressures ranging from 5 to 75 kbar.

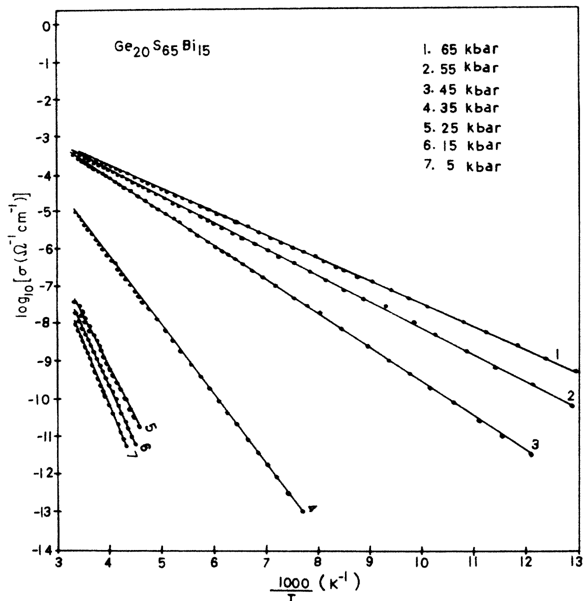

FIG. 5. Temperature-dependence conductivity of $Ge_{20}S_{65}Bi_{15}$ at pressures ranging from 5 to 65 kbar.

variation with the Bi content on either side of (25—35)-kbar pressure where there is linear decrease in ΔE with x value. Temperature dependence of conductivity in Fig. 5 for $x=15$ compositions also shows a sort of transition region from 25- to 35-kbar pressure. Similar temperature dependence of conductivity in $x=11$ composition was also observed. No such transition region appears in the data for the $x=4$ sample presented in Fig. 4. Pressure and composition dependence of the preexponential factor σ_0 shown in Figs. 8 and 9, respectively, also reveals a transition region around (25—35)-kbar pressure. Further, the dependence of σ_0 on pressure and composition in $x=0$ and 4, on the one hand, and in $x=11$ and 15, on the other hand, is distinctly different.

The typical features of the data referred to above are to be compared with the pressure dependence of resistivity in $x=0$, 4, 11, and 15 compositions presented in Fig. 1. The transition region of 25—35 kbar in the electrical parameters of these semiconductors can be easily associated with the corresponding changes in the resistivity in this region where a first sharp transition corresponding to the pressure-induced transformation

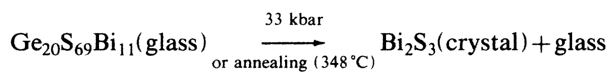

$$Ge_{20}S_{69}Bi_{11}(\text{glass}) \xrightarrow[\text{or annealing (348 °C)}]{\text{33 kbar}} Bi_2S_3(\text{crystal})+\text{glass}$$

appears.[4]

This distinct correspondence is a remarkable feature of our results. At higher pressures, the system undergoes a second structural transformation:[4]

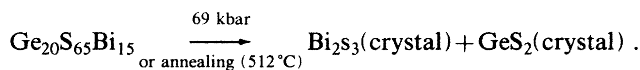

$$Ge_{20}S_{65}Bi_{15} \xrightarrow[\text{or annealing (512 °C)}]{\text{69 kbar}} Bi_2S_3(\text{crystal})+GeS_2(\text{crystal}) .$$

TABLE I. Electronic conduction data for $Ge_{20}S_{80-x}Bi_x$ ($x=0$, 4, 11, 15) semiconductors. Symbols used are explained in the text.

Composition	Quantity	Normal Pressure	5 kbar	15 kbar	25 kbar	35 kbar	45 kbar	55 kbar	65 kbar	75 kbar
$x=0$	σ ($\Omega^{-1}cm^{-1}$)	5.35×10^{-13}	3.38×10^{-13}	1.56×10^{-13}	1.61×10^{-13}	2.01×10^{-12}	3.67×10^{-11}	1.13×10^{-10}	1.78×10^{-10}	2.51×10^{-10}
	σ_0 ($\Omega^{-1}cm^{-1}$)		5.74×10^{5}	1.74×10^{2}	2.8×10^{-2}	1.1×10^{-2}	2.1×10^{-2}	5.9×10^{-3}	2.0×10^{-3}	5.8×10^{-4}
	ΔE (eV)		1.09	0.90	0.67	0.58	0.52	0.46	0.42	0.38
$x=4$	σ ($\Omega^{-1}cm^{-1}$)		6.04×10^{-11}	3.0×10^{-10}	1.49×10^{-9}	7.4×10^{-9}	3.67×10^{-8}	1.58×10^{-7}	7.94×10^{-7}	3.98×10^{-6}
	σ_0 ($\Omega^{-1}cm^{-1}$)		1.84×10^{5}	1.55×10^{4}	80.32	18.13	8.71	4.26	4.31	1.98
	ΔE (eV)		0.92	0.82	0.64	0.56	0.50	0.44	0.40	0.34
$x=11$	σ ($\Omega^{-1}cm^{-1}$)	1.24×10^{-9}	1.55×10^{-9}	3.19×10^{-9}	6.58×10^{-9}	2.47×10^{-5}	5.59×10^{-4}	5.98×10^{-4}	6.26×10^{-4}	6.6×10^{-4}
	σ_0 ($\Omega^{-1}cm^{-1}$)		4.34×10^{4}	4.36×10^{3}	37.4	209	28.06	1.37	0.143	
	ΔE (eV)		0.80	0.72	0.58	0.40	0.28	0.20	0.14	
$x=15$	σ ($\Omega^{-1}cm^{-1}$)	5.16×10^{-9}	8.85×10^{-9}	1.85×10^{-8}	2.42×10^{-8}	8.62×10^{-6}	3.05×10^{-4}	3.34×10^{-4}	3.47×10^{-4}	63.75
	σ_0 ($\Omega^{-1}cm^{-1}$)		731	249	0.024	9.585	3.230	0.076	0.035	
	ΔE (eV)		0.65	0.60	0.54	0.36	0.18	0.14	0.12	

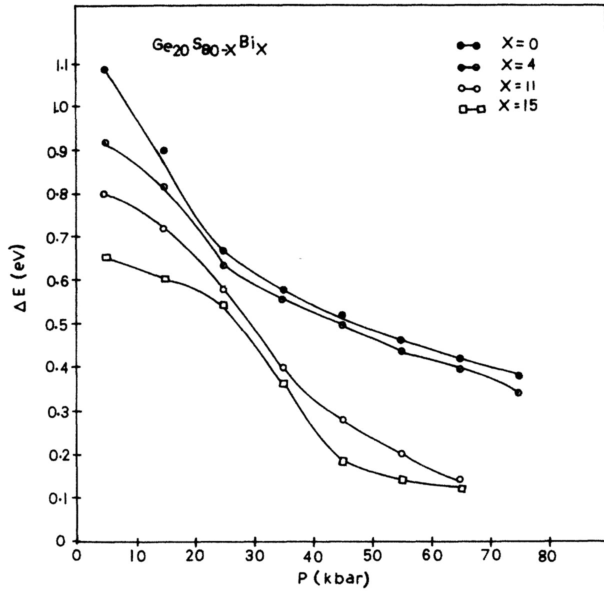

FIG. 6. Pressure dependence of activation energy ΔE of $Ge_{20}S_{80-x}Bi_x$ at $x=0$, $x=4$, $x=11$, and $x=15$.

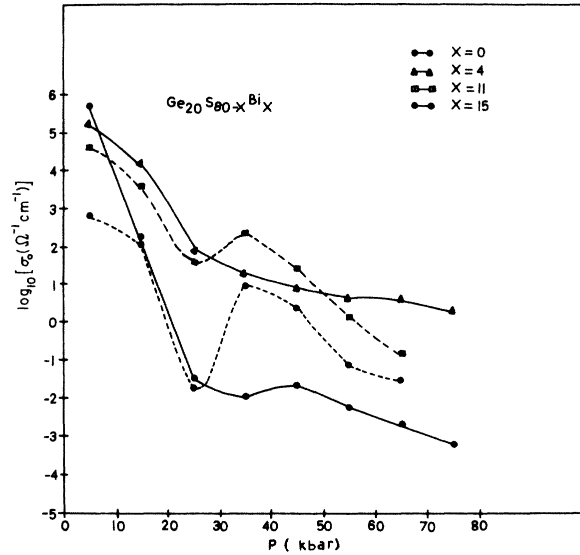

FIG. 8. Pressure dependence of preexponential factor σ_0 in four compositions: $x=0$, $x=4$, $x=11$, and $x=15$.

IV. DISCUSSION

A. Structural model

Germanium chalcogenide glasses can be described as small chemically ordered clusters embedded in a continuous network as proposed by Phillips.[13] In Ge_xS_{1-x} glass, some of these clusters are $(S)_n$ chains, $Ge(S_{1/2})_4$ corner sharing tetrahedral, and $Ge_2(S_{1/2})_6$ ethanelike structural units which dominate Ge_xS_{1-x} alloys near $x=0$, 0.33, and 0.4, respectively. In the S-rich region the first two types of clusters would dominate. Further, according to Phillip's model, the structural element in a-GeS_2 is an outrigger raft representing a large cluster of atoms. This cluster is a strongly associated mixture of large chalcogenide-rich outrigger rafts and small Ge-rich ethanelike units with the proportions adjusted to achieve overall stoichiometry. Both kinds of clusters are locally linearly polymerized and the rafts are locally stacked.

We make this Phillip's structural model a basis for discussion of the structural aspects of Bi-doped glasses studied in this work. When Bi is added to sulfur-rich glass $Ge_{20}S_{80-x}Bi_x$, it significantly modifies the amorphous network of the host glass, particularly at higher impurity concentration. We propose that at low Bi concentration $(x=4)$ the impurity seems to enter mostly into $(S)_n$

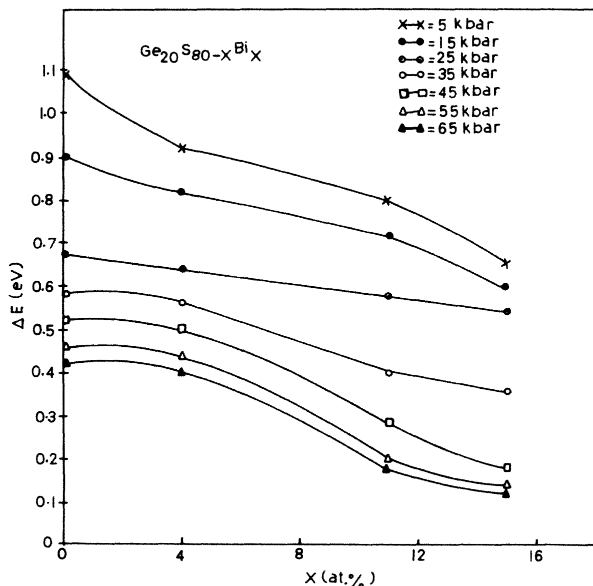

FIG. 7. Composition dependence of activation energy ΔE at pressures ranging from 5 to 65 kbar.

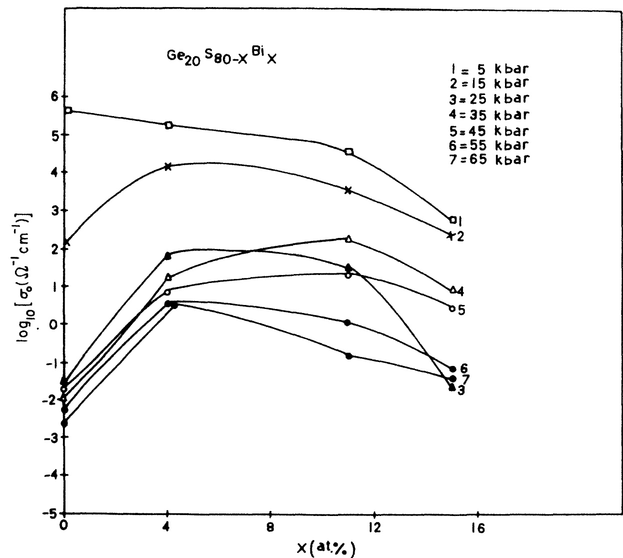

FIG. 9. Composition dependence of preexponential factor σ_0 at pressures ranging from 5 to 65 kbar.

chains connecting the tetrahedral units and will thus make Bi—S bonds. Such type of substitution is not expected to affect drastically either the structure or the overall cohesion of the alloys. At higher Bi concentrations ($x=11,15$) the impurity atoms possibly penetrate into the $Ge(S_{1/2})_4$ tetrahedra, making complex Ge-Bi-S clusters containing all the three constituent atoms, and possibly making a Ge—Bi bond. Such an entry of Bi would considerably modify the host amorphous network. These proposals get support from the pressure-induced effects in the electrical transport in these glasses presented in Figs. 1–5. The behavior of $x=4$ composition under pressure is drastically different from that of $x=11$ and 15 compositions, indicating considerable structural modifications at higher impurity concentrations. Such a modified glass upon heating or under high pressure undergoes structural transformations, and the clusters decompose and crystallize into the smaller units Bi_2S_3 and GeS_2 as revealed in our earlier investigations.[4] The crystallized phases have been identified by x-ray diffractometry and by differential thermal analysis in our earlier paper.

To further understand the chemical bonding in the clusters, Ge-Bi-S in the amorphous material, the approach of Tichy *et al.*[14,15] regarding bond statistics in germanium chalcogenide glasses is taken into account. Moreover, it has also been recently found that Bi atoms enter into amorphous Bi_2X_3 ($X=$S, Se) in threefold coordination.[16] If we accept that Bi also enters into amorphous $Ge_{20}S_{80}$ in threefold coordination at all concentrations, then the proposed bonding arrangement in the clusters can be visualized as in Fig. 10. At lower Bi concentrations mostly, the bonding arrangement of Fig. 10(a) is preferred by the system, by dissolution of Bi in sulfur chains. As Bi concentration is increased atomic arrangements, as shown in Figs. 10(b) and 10(c), are developed. Therefore, at large Bi concentrations, clusters containing all three atoms (Ge, Bi, and S) are preferred. Such substitution of the added Bi atoms would considerably modify the glassy network as supported by the observed pressure-induced effects in the doped semiconductors presented in Sec. III.

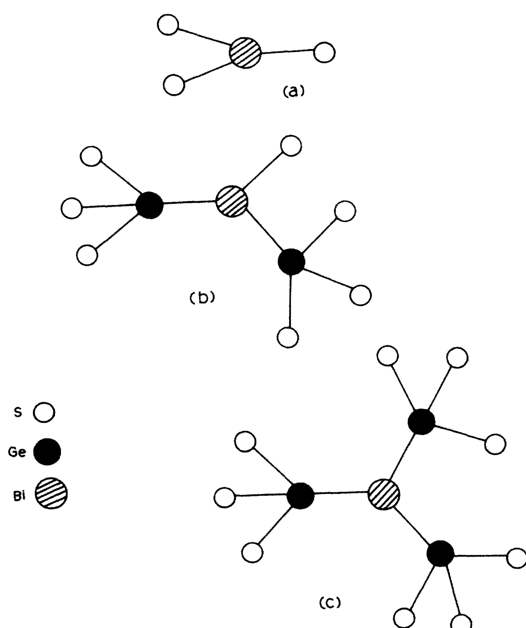

FIG. 10. Possible bonding arrangement in $Ge_{20}S_{80-x}Bi_x$.

It is of relevance to compare this feature of Bi dopants in Ge-S glass with that of Sb dopants in Ge-S glass.[15] In the case of Sb-doped Ge-S, glass clusters of type (a) are preferred at all Sb concentrations, thus forming SbS_3 units. This quite different behavior in Ge-S glass of two dopants Bi and Sb belonging to the same group of the Periodic Table is quite interesting. Further, Bi dopants in Ge-S changes the carrier sign from p type to n type whereas Sb dopant does not reverse the carrier sign.

B. Defect centers

In this section we first present briefly the nature of defects in Ge-S glasses. The presence of characteristic negative-correlation-energy charged defects in a variety of chalcogenide glasses is quite well established.[17–20] A negative correlation energy U occurs when the reaction

$$2D^0 \rightarrow D^+ + D^-$$

is exothermic where D^+, D^-, and D^0 represent the possible threefold coordinated C_3^+, singly coordinated C_1^- charged defects, and singly coordinated neutral defect C_1^0, respectively. The characteristic properties generated by these defects are a pinned Fermi energy, diamagnetism, trap-limited transport of the majority carrier, etc.[21] Departure from the ideal behavior may be caused either by the presence of additional states in the gap or by the primary defects in fact having a positive U. In S (Se) the defects are C_3^+ and C_1^-. In the case of compound amorphous semiconductor such as GeS_2, the defect structure becomes more complex because other types of defects with similar properties are possible. Moreover, the effect of ionicity[18,21] on the defect structure introduces further complications. The main consequence of ionicity is that heteropolar bonding is the lowest-energy configuration, and therefore the compounds are chemically ordered. Following arguments of Street and Lucovsky in Ref. 21, the alloy glass GeS_2 contains $C_1^-(T_1)$ and an equal number of $C_3^+(T_3)$ defects. The lowest-energy C_3^+ center is bound to three Ge atoms in a configuration denoted by $C_3^+(T_3)$. Similarly the center C_1^- is bound to one Ge atom in a configuration $C_1^-(T_1)$. $C_3^+(T_3)$ is shown to be unable to convert into $C_1^-(T_1)$; hence it should have a positive correlation energy U. On the other hand, $C_1^-(T_1)$ defect can convert into $C_3^+(T_2C_1)$, and has a negative correlation energy. $C_3(T_3)$ is an electron trap and $C_1^-(T_1)$ is a hole-trap type of defect. The resulting states in the gap are shown in Fig. 11. In this model the doping by shallow donors and acceptors is possible. The addition of donors immediately fills level A, and the Fermi level moves up to this energy. On the other hand, acceptors merely convert $C_1^-(T_1)$ into $C_3^+(T_2C_1)$ and so the Fermi energy is unchanged. Thus, there is pinning of E_F only in one direction. This particular aspect of germanium chalcogenides makes them unique bulk glasses.

We take into account the above details of defects in germanium chalcogenide glasses in discussing the effect of Bi

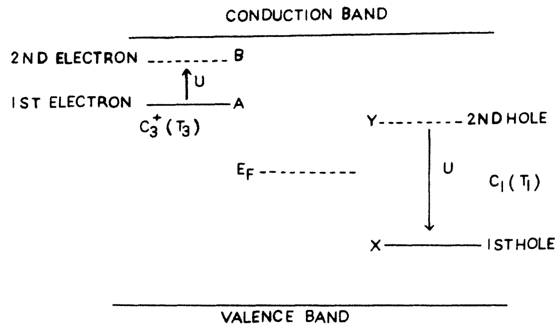

FIG. 11. Electronic states of the $C_1(T_1)$ defects with negative U, and $C_3^+(T_3^+)$ defect with positive U. In the low-temperature equilibrium the electron trap A and the hole-trap X are unoccupied, and therefore the two-particle states B and Y are inaccessible. E_F is position of Fermi level.

dopants on these glasses. It has also been observed by photoemmission studies[16] that in amorphous Bi_2S_3 films Bi atoms are threefold coordinated. Moreover, the electronegativity (EN) of S with an (EN of 2.5) is greater than that of Bi with an (EN of 2.0). Accordingly, a shift of electron density from Bi to S is expected to occur. This indicates that the Bi atoms in Bi_2S_3 are positively charged ($Bi_2{}^{+\delta}$ $S_3{}^{-\delta}$). We propose that addition of Bi into $Ge_{20}S_{80-x}Bi_x$ in smaller concentration leads mostly to the formation of $P_4^+(C_4)$ and $C_1^-(P_1)$ charged defects as in As_2Se_3. Here "P" stands for pnictide (Bi belongs to this category). Therefore positive and negative defects are centered at Bi and S, respectively. Since Ge-S-Bi glasses at low Bi content (<11 at. %) exhibit p-type conduction, addition of Bi into the system merely converts defects like $C_1^-(T_1)$ into $C_3^+(T_2C_1)$ without changing the position of the Fermi level. However, at large Bi concentration ($x \geq 11$ at. %) the dopant introduces network modification and positive correlation energy defects like $C_3^+(T_3)$ present in the parent Ge-S glass are converted into $T_3^-(C_3)$ thus shifting the Fermi level towards the conduction band. This seems to be the unique property of Bi dopants.

C. Electronic conduction

Electronic transport data presented in Sec. III can be discussed on the basis of a thermally activated conduction process in extended states and/or localized states of the semiconductor. Temperature-dependent conductivity in all the samples at various pressures is in good agreement with exponential law giving one activation energy in the whole temperature range.

The conduction takes place due to the electrons and/or holes excited into the extended states in the conduction and/or valence band near the mobility edge which is represented by the equation of the form[22]

$$\sigma=\sigma_0 \exp[-(E_c-E_F)/k_B T] \qquad (2)$$

for electron conduction, where $E_c-E_f=\Delta E$ varies linearly with the temperature as $E_c-E_f=E(0)-\gamma T$. $E(0)$ is the energy distance between mobility edges at $T=0$ K. Here

$$\sigma=\sigma_{01} \exp\left[\frac{\gamma}{k_B}\right] \exp\left[\frac{-E(0)}{k_B T}\right] .$$

The value of σ_{01} for chalcogenide semiconductors is between 10 and 10^3 $\Omega^{-1}\,\mathrm{cm}^{-1}$. The value of the temperature dependence of the optical gap generally lies between 1×10^{-4} and 8×10^{-4} eV/deg. The value of γ is about half this value. Therefore, $\exp\gamma/(k_B)$ lies in the range 10–100. A plot of $\log_{10}\sigma$ and $1/T$ gives the slope E_c-E_f and $\sigma_0=\sigma_{01}\exp(\gamma/k_B)$.

We have utilized the above concepts to determine the values of σ_0 and ΔE which are included in Table I for various compositions. Following Mott and Davis[23] the value of σ_0 in the range 10^3–10^4 $\Omega^{-1}\,\mathrm{cm}^{-1}$ in chalcogenide glasses indicates that conduction is in the extended states. A smaller value of σ_0 indicates the presence of a wide range of localization and conduction by hopping in the localized states. It is clear from Table I that large values of σ_0 at lower pressures suggest the major contribution from extended state conduction. As the semiconductor is subjected to increasing pressures, the Fermi level moves towards the mobility edge (towards conduction band in case of n-type material) and an increasing number of carriers become available in the localized states in the band tails where the phonon-assisted hopping takes place. This is illustrated by the very small values of the preexponential factor σ_0 at higher pressures in Fig. 8. Correspondingly, the pressure and composition dependence of ΔE as shown in Fig. 6 and 7, respectively, indicates that the decrease of the energy gap increases the number of carriers available for conduction. This should include two contributions: (i) movement of the Fermi level towards the mobility edge, and (ii) the pressure-induced decrease in the energy gap of the semiconductor which is a molecular solid having clusters instead of being a continuous random network solid. It is known that[24] for less than three-dimensional network materials, compression mainly forces the molecular clusters closer together without affecting nearest-neighbor distances. The fundamental absorption edge in molecular solids like germanium chalcogenide glasses red shifts strongly to lower energy with increasing pressure.[24] This aspect of the germanium chalcogenide glasses studied in the present investigation contributes towards the electrical conduction.

An interesting aspect of our results is that around 30-kbar pressure, where first transition takes place, the values of parameters ΔE, σ_0, and σ show a distinct change. Our earlier results of x-ray diffraction established[4] that a pressure-induced crystallization of $x=11$ and 15 compositions into Bi_2S_3 (crystals) takes place around 33 kbar along with a drop in the resistivity by about 6 orders of magnitude. Figure 5 shows the temperature-dependent conductivity of the composition $x=15$, clearly illustrating the effect of crystallization. Microcrystals of Bi_2S_3 are uniformly dispersed in the background glassy matrix. The system becomes a fine ceramic glass. Nonappearance of crystalline Bi_2S_3 in $x=4$ composition is attributed to the compactness of the glassy composition and the presence of a simpler structural unit in the glass. Presence of microcrystals of Bi_2S_3 in $x=11$ and 15 compositions at a pressure of 25 kbar induces a much faster decrease of ac-

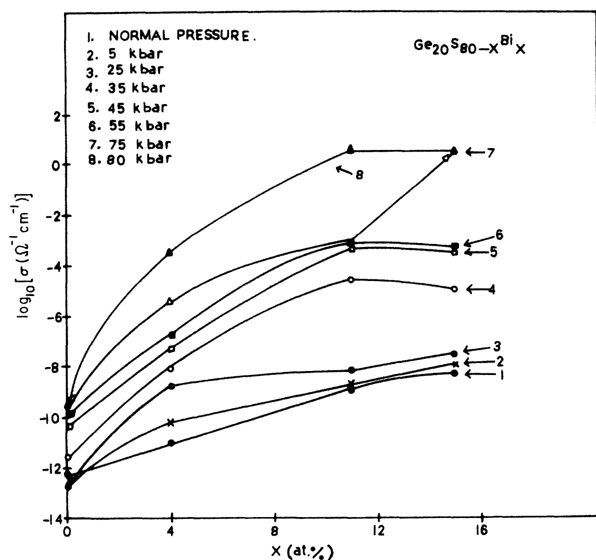

FIG. 12. Composition dependence of the conductivity (at 300 K) at different pressures.

tivation energy ΔE with pressure, as shown in Fig. 6 for the $x=15$ sample. Concentration dependence of the conductivity σ presented in Fig. 12 shows an interesting feature that the conductivity keeps on increasing up to $x=11$ at all pressures and then there is no further appreciable increase in the composition $x=15$. This suggests that chemical modification being induced by the added impurity reaches completion at the $x=11$ value and the system becomes ready for the reversal of carrier sign. An interesting point to be noticed is the value of room-temperature conductivity σ (300 K) in $x=0$, 4, 11, and 15 samples. The maximum pressure-dependent variations (8 orders of magnitude in the pressure range studied) in the $x=4$ composition as compared to the $x=0$ sample indicates the sensitiveness of the Bi impurity-induced defect centers in the host network of $Ge_{20}S_{80}$ glass. Incorporation of Bi up to 4 at. % leads to a relatively great change in the optical-absorption edge.[3] At higher concentrations, there is little change in the optical-absorption edge. This is a clear indication of incorporation of Bi in creating tail states for lower concentrations. At higher concentrations, there is a good possibility of network modification. In $x=11$ and 15 compositions, there is very little change in σ (300 k) up to 25-kbar pressure. Then after the first phase transition, there is again very little change in σ (300 K) up to 65-kbar pressure.

To attempt a more complete and quantitative interpretation of our experimental results, the pressure dependence of conductivity mobility and Hall mobility will be needed.

V. CONCLUSIONS

In conclusion, we have undertaken a systematic study of the electrical transport in Bismuth-doped n-type amorphous germanium sulfide semiconductors under high pressure and at low temperature for the first time, which has revealed the compositional dependence of the electronic conduction process in this class of doped semiconductors. This material exhibits thermally activated electronic conduction at all pressures in all the compositions. It is concluded that Bi-doped semiconductors form complex molecular clusters at large Bi concentration, involving all three elements Ge, Bi, and S. There is remarkable resemblance between the thermally activated electronic conduction under high pressure, the x-ray diffraction studies of pressure quenched compositions, and the results of differential thermal analysis. It is proposed that the n-type conduction in Bi-doped germanium chalcogenides with large concentration of the dopant is due to the participation of the Bi impurities in attacking the positive correlation energy defects found in germanium chalcogenides which leads to the movement of the Fermi level away from its pinned position towards the conduction-band mobility edge. At lower impurity concentrations, the added dopant influences only the negative correlation energy defects.

ACKNOWLEDGMENTS

This work was supported by the Department of Science and Technology and by the Department of Atomic Energy (Government of India). The authors express their gratitude to these agencies. One of us (K.L.B.) gratefully acknowledges a gift of instruments given by the Alexander Von Humboldt Foundation (Bonn, Federal Republic of Germany). Technical assistance of Sh.N.K.Abbi is acknowledged. G.P. and E.S.R.G. thank the Defense Research and Development Organization (DRDO) scheme (Government of India) for financial support.

[1]K. L. Bhatia, G. Parthasarathy, and E. S. R. Gopal, J. Phys. Chem. Sol. **45**, 1189 (1984).

[2]K. C. Tai, W. R. Sinclair, R. G. Vadimsky, and J. M. Moran, J. Vac. Sci. Technol. **16**, 1977 (1979).

[3]P. M. Nagels, L. Tichy, A. Triska, and H. Ticha, J. Non-Cryst. Solids **59-60**, 1018 (1983).

[4]D. P. Gosain, K. L. Bhatia, G. Parthasarathy, and E. S. R. Gopal, Phys. Rev. B **32**, 2727 (1985).

[5]K. L. Bhatia, G. Parthasarathy, and E. S. R. Gopal, J. Non-Cryst. Solids **59-60**, 1019 (1983).

[6]K. L. Bhatia, G. Parthasarathy, E. S. R. Gopal, and A. K. Sharma, Solid State Commun. **51**, 739 (1984).

[7]K. L. Bhatia, G. Parthasarathy, and E. S. R. Gopal, J. Non-Cryst. Solids **69**, 189 (1985).

[8]K. L. Bhatia, G. Parthasarathy, D. P. Gosain, and E. S. R. Gopal, Philos. Mag. B **51**, L63 (1985).

[9]K. L. Bhatia, G. Parthasarathy, D. P. Gosain, A. K. Sharma, and E. S. R. Gopal, J. Mater. Sci. Lett. **5**, 181 (1986).

[10]K. L. Bhatia, J. Non-Cryst. Solids **54**, 173 (1983); **58**, 151 (1983).

[11]A. K. Bandyopadhyay, A. V. Nalini, E. S. R. Gopal, and S. V. Subramanyam, Rev. Sci. Instrum. **51**, 136 (1980).
[12]H. Kokado, I. Shimizu, and E. Inoue, J. Non-Cryst. Solids, **20**, 131 (1976).
[13]J. C. Phillips J. Non-Cryst. Solids **55**, 179 (1983).
[14]L. Tichy, A. Triska, C. Barta, H. Ticha, and M. Frumar, Philos. Mag. B **46**, 365 (1982).
[15]L. Tichy, H. Ticha, M. Friomar, J. Klikorta, A. Triska, C. Brorta, and A. Nemecokova, Czech. J. Phys. B **32**, 1363 (1982).
[16]T. Takahashi, T. Sagawa, and H. Hamanake, J. Non-Cryst. Solids **65**, 261 (1984).
[17]N. F. Mott. Philos. Mag. **34**, 10 (1976); **51**, 177 (1985).
[18]J. Robertson, Philos. Mag. **51**, 182 (1985).
[19]S. R. Elliott and E. A. Davis, **12**, 2577 (1979).
[20]D. Adler, Sol. Cells **2**, 199 (1980).
[21]R. A. Street and G. Lucovsky, Solid State Commun. **31**, 289 (1979).
[22]P. Nagels, in *Amorphous Semiconductors*, edited by Editors (Springer, Berlin, 1979) Vol. 36, p. 133.
[22]P. Nagels, in *Amorphous Semiconductors*, edited by M. H. Brodsky (Springer, Berlin, 1979) Vol. 36, p. 133.
[24]R. Zallen, B. A. Weinstein, and M. L. Slade, J. Phys. (Paris), Colloq. **42**, C4-241 (1981).